Validation of BS 7910 fracture assessment procedures; Wide Plates and Cylinders

Konstantinos Kouzoumis[1,2,*], Isabel Hadley[1,3], Mahmoud Mostafavi[1]

[1] University of Bristol, Queens Building, University Walk, BS8 1TR, Bristol, UK

[2] NSIRC, Granta Park, Great Abington, CB21 6AL, Cambridge, UK

[3]TWI Ltd, Great Abington, Cambridge, UK, CB21 6AL

Abstract

BS 7910 provides guidance on the fitness for service of a flawed component. It covers a wide variety of metals in broad applications, thus the integrity of many components in various safety critical industries depends on it. Its detailed and rigorous validation, therefore, is of utmost importance. In this study, validation of the fracture assessment procedures of BS 7910 is carried out through the use of historical large test data, where the failure conditions are known in detail. Hundreds of test results from large-scale wide plate and cylinder tests are collected from the literature and assessed with BS 7910. The outline of the analysis and the tests analysed are given in this study in a concise manner. The exercise validates the fracture clauses and associated annexes that concern plate, pipe and curved shell geometries, together with other equations included in the procedure and used during the analyses.

1. Introduction

Fitness for Service (FFS) Procedures, like BS 7910 [1], R6 [2] and API 579-1/ASME [3] are built upon sound fracture mechanics principles and engineering data, and have been implemented by the engineering community for many decades. They provide guidance on conducting Engineering Critical Assessments (ECAs) for purposes ranging from defect-tolerant design to life extension of safety-sensitive components.

The formulae used for the necessary calculations during an ECA can vary in terms of accuracy between different procedures and especially when considering the wide variety of applications that each of them has to cover. In order to ensure that the FFS procedures can provide acceptable results in all these different applications they need to be validated regularly. Validation is achieved by applying them in situations in which the failure conditions are known. For example, a large-scale test, in which the loading history, geometric parameters and mechanical properties, are known, could be used. Assessments of such tests with the use of an FFS procedure demonstrate if it is reliable and can help trace potential inadequacies or room for improvement.

Validation is therefore an important tool that is applied to standards to improve their existing accuracy and to safely incorporate new additions to them, e.g. consideration of the effect of constraint on failure [4]. Validation against experimental data ensures that standards encapsulate best practice that's calibrated to real cases, nevertheless validation is often done using finite element analyses (FEA) [5], [6] or a combination of FEA and experiments [7].

* Corresponding author. E-mail address: k.kouzoumis@bristol.ac.uk

Experimental validation work for FFS standards is very limited in the public domain. Even though updated versions of standards are usually followed by overview papers explaining the newest alterations [8]–[13], widely used standards like R6 [2] and API 579-1/ASME [3] include most of their experimental validation work inside the standard (API 579-1/ASME - Annex H, R6 – Chapter V). In the cases where information is included in other sources these are usually in bulletins/reports [14]–[16] and not in the public domain.

In order to update the limited experimental validation data available in the public domain and to evaluate the accuracy of the procedure, a validation exercise of BS 7910, including analysis of several hundred large-scale fracture tests from the literature, has been conducted.

The exercise was initially carried out with the use of the 2013 version of the standard [17], which was the most recent at the time, while all assessments in this study are Option 1 assessments, as explained in detail in Section 2. An important result of the analyses with 2013 version was to investigate an aspect for modification for the newest version (2019) of BS 7910 [1]. This concerned the proximity to plastic collapse (L_r) of a pipe (or curved shell) containing an axial flaw, either surface-breaking or through thickness. Namely, the reference stress solutions used for the calculation of L_r were found to be overconservative, due to a multiplication factor. As explained in [18], this factor provides added conservatism thus not being necessary for a safe assessment and has been omitted in the 2019 version of BS 7910 [1]. Detailed assessments with and without this factor can be found in Appendix 1 of the report that contains all original assessments [19].

This paper focuses on the stress based assessment of full scale tests on plates as well as pressure vessels and pipelines (cylinders/curved shells), some of which have been studied in the past with earlier versions of BS 7910 [14], [20]–[22], to check the soundness of the latest version [1] and to make recommendations, where appropriate, to improve the applicability of the procedure. For the cases that have been assessed in previous work, all original sources mentioned will be assessed directly and reanalysed when possible, while where the original reports are not available the data will be selected from previous validation work [21]–[23].

In pursuit of conciseness an overview of the work conducted is presented in this paper, whilst the Appendix 1 of the TWI member report [19] with all the detailed analyses is available upon request in case the reader requires further details. The following section is an outline of the background of the analyses. The basic steps taken during an ECA are presented together with the required information/values needed for it. The equations and guidance employed from BS 7910 for the calculation of these values are also given. This is followed by the presentation of the test database gathered from literature and the results of the analyses.

2. Background to Analyses

An ECA is represented graphically with the use of the Failure Assessment Diagram (FAD). This consists of a failure assessment line (FAL) and the assessment point of the component analysed. The FAL divides the diagram into two zones, i.e. underneath/inside the FAL and outside the FAL. The zone inside is considered as the “acceptable/safe region” while the one outside is the “unacceptable/potentially unsafe region”. Depending on where the assessment point lies, the flaw is deemed as acceptable, i.e. the component can withstand the loading conditions modelled, or unacceptable, i.e. its integrity cannot be guaranteed. A graphical representation of a FAD can be found in Figure 1.

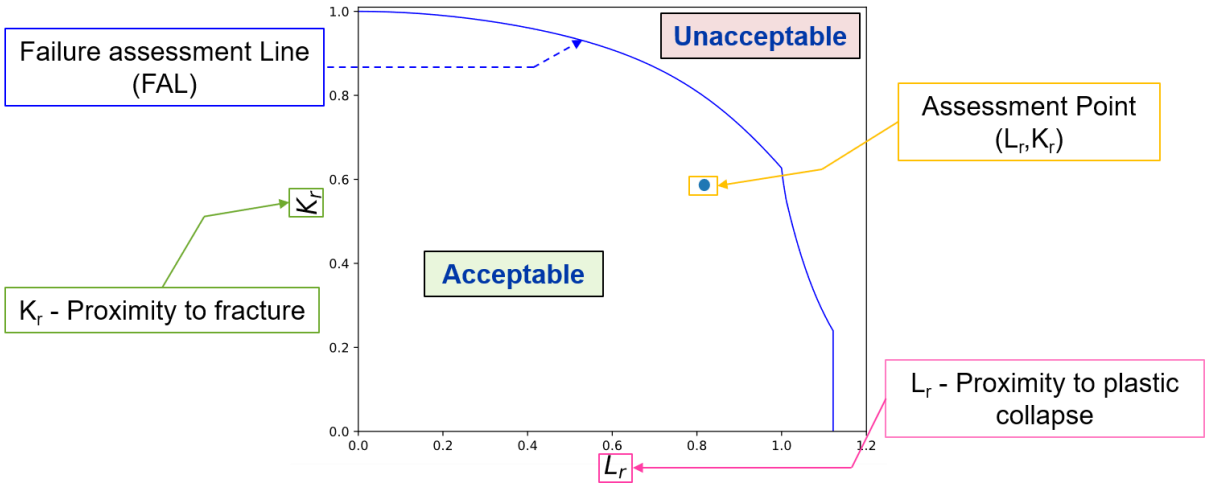

Figure 1: Graphical presentation of an ECA

There are three assessment options (Option 1 – 3); with increasing option number the FAL is more accurate and less conservative but requires a higher amount of information for its calculation. In this study only Option 1 assessments are made, due to the limited data available in most cases. The Option 1 FAL requires knowledge of the yield stress (σ_y) and tensile strength (σ_{UTS}) of the material as well as its yielding behaviour (continuous/discontinuous yielding). In many cases where σ_y, σ_{UTS} are not available at the test/operating temperature, they were determined following the guidance the standard provides for calculation of the tensile properties at different temperatures in clause 7.1.3.4 [1] background for this clause is provided in [24].

The assessment point is plotted with an abscissa designated L_r, considered as proximity to plastic collapse, and an ordinate of K_r, proximity to fracture. Their values are calculated from the following equations,

$$L_r = \frac{\sigma_{ref}}{\sigma_y} \qquad \text{Equation 1}$$

$$K_r = \frac{K_I^p + K_I^s}{K_{mat}} + \rho \qquad \text{Equation 2}$$

Where:

- σ_{ref} : the reference stress calculated in accordance with Annex P
- K_I^p, K_I^s: the elastic stress intensity factor at the current crack size due to primary and secondary stresses respectively, calculated in accordance with Annex M
- ρ: a function of primary and secondary loads that account for plasticity interaction effects, calculated according to Annex R
- K_{mat}: the 'characteristic' (i.e. lower bound) fracture toughness. This was given directly in terms of a critical stress intensity factor (MPa√m), or J-integral (kJ/m^2) value converted to stress intensity factor (K_J); in many cases it was estimated from Charpy measurements (J), using the guidance of Annex J.

In some cases, where the material of the tested specimen exhibited tearing under increasing load, the original reports provided fracture tearing resistance curves (R-curve). In these instances, various amounts of ductile tearing were postulated (from 0.2 to 2 mm) and L_r and K_r were calculated at different flaw sizes equivalent to the initial flaw length plus the postulated amount

of crack growth. The fracture ratio (K_r) was calculated using an enhanced K_{mat} which corresponded to the postulated amount of tearing. This resulted to each specimen having a series of L_r, K_r value pairs as a function of increasing flaw size. These were plotted on the FAD as a line consisting of the locus of the assessment points that derive from the different flaw lengths. An example of what an assessment including ductile tearing resistance (R-curve) looks like is given in Figure 2, where the locus of assessment points lies in the unsafe zone of the FAD.

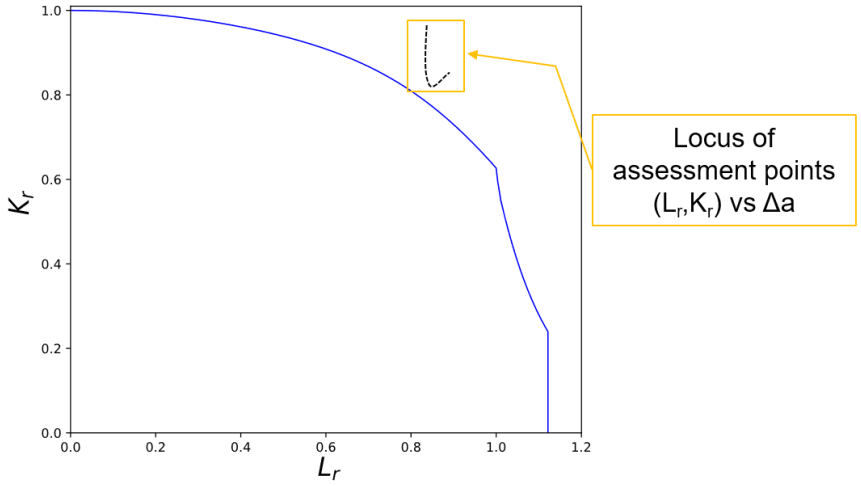

Figure 2: Example of tearing resistance (R-curve) assessment

The geometries studied in this exercise are wide plates and closed cylinders/pipes. The annexes in BS 7910 that address reference stress and stress intensity factor solutions are Annex P and Annex M accordingly. Table 1 includes the subclauses of the annexes the solutions were obtained from, while further information concerning the origin of the solutions can be found in [25]. In Table 1 "closed cylinders" refer to the geometry of pipes/closed cylinders (i.e. cylindrical pressure vessels), while curved shells refer to flat plates with curvature. It should be noted that several of the tested pipes had geometrical features which exceeded the validity margins of the stress intensity factor solutions for closed cylinders and were assessed as curved shells.

Table 1: Reference stress and Stress intensity factor solutions used for the assessments

Component Geometry	Flaw Geometry		Reference Stress Solution	Stress Intensity Factor solution
Wide Plate	Surface Cracked Tension (SCT)		P.5.1	M.4.1
	Centre Cracked Tension (CCT)		P.4.1	M.3.1
	Extended Surface Crack Tension (ESCT)		P.5.2	M.4.3
Closed Cylinder	Axial Flaws	External Surface (AES)	P.8.4	M.7.2.4
		Through Thickness (ATT)	P.8.1	M.7.2.1
	Circumferential Flaws	External Surface (CES)	P.9.4	M.7.3.4
		Through Thickness (CTT)	P.9.1	M.7.3.1
Curved Shell	Axial Flaws	Internal Surface (AIS)	P.8.2	M.6
		External Surface (AES)	P.8.4	M.6
	Circumferential Flaws	Internal Surface (CIS)	P.9.2	M.6

Concerning the reference stress solutions used for the assessment of axially flawed cylinders or curved shells (Clause P.8.1, P.8.2, P.8.4), the 2013 version of BS 7910 included a multiplication factor of 1.2

on the membrane stresses. As explained in [18], this factor provides added conservatism thus not being necessary for a safe assessment and is omitted in the 2019 version and here from the reference stress solutions implemented in the analyses of axially flawed cylindrical geometries. Detailed assessments with and without this factor can be found in [19].

Regarding tensile properties they were in many cases given at room temperature rather than the temperatures at which the specimens were tested. Clause 7.1.3.4 provides guidance for the estimation of the properties at the correct temperatures and was used as follows.

- For tests conducted above room temperature the yield stress de-rating graph shown in Figure 3 combined with the yield stress to ultimate tensile strength ratio were used to calculate the corresponding properties.
- For tests conducted below room temperature the yield stress and ultimate tensile strength were translated from the room temperature properties using Equation 3 and Equation 4 respectively.

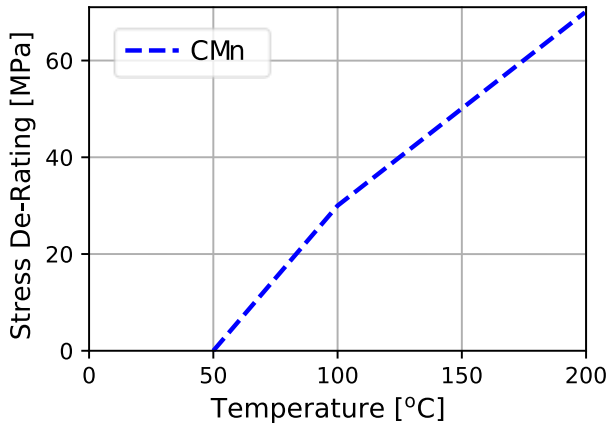

Figure 3: Yield Stress De-rating for C-Mn Steels. Adapted from [1, Fig. 7.10]

$$\sigma_{y\ (Test\ temperature)} = \sigma_{y\ (\ room\ temperature)} + \frac{10^5}{(491 + 1.8\mathrm{T})} - 189 \qquad \textit{Equation 3}$$

$$\sigma_{UTS\ (Test\ Temperature)} = \sigma_{UTS\ (room\ temperature)} \times \left(0.7857 + 0.2423 exp\left(-\frac{\mathrm{T}}{170.646}\right)\right) \qquad \textit{Equation 4}$$

Where T is the temperature (in ˚C) at which the properties are calculated. This guidance is of empirical nature and supporting evidence for its origin and validity are given in [24].

Some of the original reports of the axially flawed pipes provided Charpy impact test values rather than valid fracture toughness measurements. A conservative estimate of K_{mat} can be calculated from Charpy measurements with the use of Annex J, where equations based on the empirical correlation of the two are given. The equations used from the annex in this study are given here as Equation 5 and Equation 6, while background for these can be found in [24] and [26]. The latter was used for low sulphur steels on the upper shelf and provides a fracture toughness estimate at 0.2mm of ductile crack extension, thus calculating $K_{mat0.2}$.

$$K_{mat} = 0.54C_v + 55 \qquad \textit{Equation 5}$$

$$K_{mat0.2} = K_{J0.2} = \sqrt{\frac{E(0.53C_{Vus}^{1.28})\left(0.2^{0.133C_{Vus}^{0.256}}\right)}{1000(1-v^2)}} \qquad \textit{Equation 6}$$

Where C_v is the lower bound Charpy V-notch impact energy at the temperature for which K_{mat} is being calculated, C_{Vus} is the upper shelf energy

In the cases where residual stresses were included, these were treated according to the guidance of Clause 7.1.10. In five analyses (Specimen ID: 2540, 2541, 2546-2548 in Table 2), where there were enough information available, non-uniform residual stress profiles were included with the use of the annex that provides guidance on residual stress profiles for assessing flaws in as-welded joints (Annex Q) . The rest of the welded specimens were studied assuming a uniform stress profile. For the as-welded specimens, the residual stresses were calculated with Equation 7, while for the post-weld heat-treated (PWHT) they were estimated with respect to flaw orientation and heat treatment parameters from Clause 7.1.10.3, which deals with residual stresses of PWHT structures. Further explanation of the guidance the standard provides on residual stresses can be found in [27].

$$Q_m = min\left[\sigma_Y', \left(1.4 - \frac{\sigma_{ref}}{\sigma_f'}\right)\sigma_Y'\right] \qquad \textit{Equation 7}$$

Where Q_m is the membrane residual stress, σ_Y' and σ_f' are the yield stress and flow strength of the parent material respectively and σ_{ref} is the calculated reference stress.

The current exercise validates all the above parameters that are calculated during ECA as well as their synergy with each other.

3. Tests Analysed

The assessments in this study have been conducted on wide plates and closed cylinders. All of the wide plates were loaded in tension. The cylinders were in most cases closed with end caps and loaded under internal pressure, while in other cases had tensile or bending loads applied. The flaw geometries included in the study consist of surface breaking flaws and through thickness flaws. A schematic of the wide plate test geometries can be found in Figure 4 , while the cylinder flaw geometries are shown in Figure 5.

Additionally, each test analysed has been given an ID which is in line with the overall validation exercise conducted within TWI. A summary of the tests analysed and their respective IDs, is shown in Table 2, where the tests have been categorized by specimen geometry and source from which their data was gathered. The test data were collected from their original reports, where possible, while for some cases for which the reports could not be retrieved, the data was taken as reported in previous validation work [3],[4],[23].

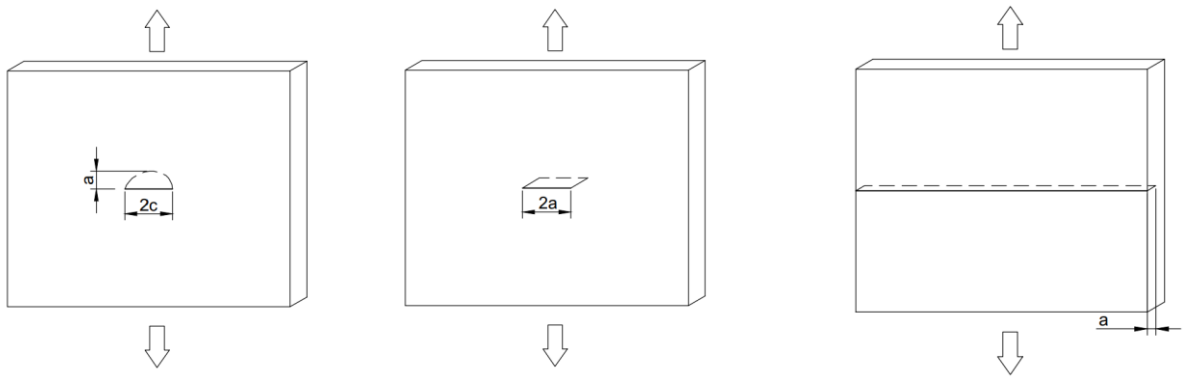

(a) Surface Crack Tension (SCT) *(b) Centre Crack Tension (CCT)* *(c) Extended Surface Crack Tension (ESCT)*

Figure 4: Wide Plate Tests Geometry

Overall there are 212 tests included in the analyses. Thirty-seven (37) of the tests concern wide plates while the rest of the specimens (175) were of cylindrical geometry.

In some cases, the geometry of the pipe lay outside the geometrical limits of K solutions for cylinders, given in BS 7910. These limits concern either the component or flaw dimensions and margins vary according to flaw orientation. In these cases, curved shell solutions were used instead. For each flaw geometry and respective cylinder equation, the limiting validity parameters and the specimens which do not comply with the margins along with the parameter value of these specimens are shown in Table 3, where B and ri refer to the thickness and the internal radius of the specimens respectively. Oriented per ID and reference, Table 4 includes the cylindrical specimens which were assessed as curved shells.

It should be noted that, out of the 37 wide plate tests analysed, 12 did not reach failure during testing and one was not certain to have failed, however they have been included in the analyses.

Further details about each set of tests examined including, their material, geometric properties and loading conditions, as well as the interpretation and implementation of this data is given in the member report [19] where all the original assessments are included. It is pointed out that the original report includes data that would be more properly analyzed with the newest addition of Annex V of the standard that includes a strain-based assessment technique. Given that this exercise was initially done with the 2013 version that data has been filtered out here. This filtering has exluded all specimens whose applied stress to yield stress ratio was higher than 1.1.

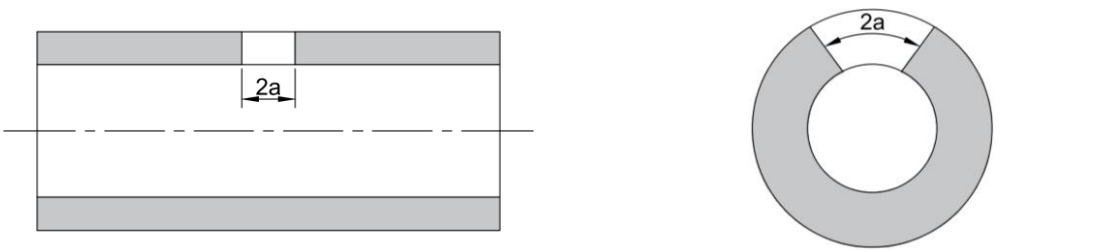

(a) Axial Through Thickness *(d) Circumferential Through Thickness*

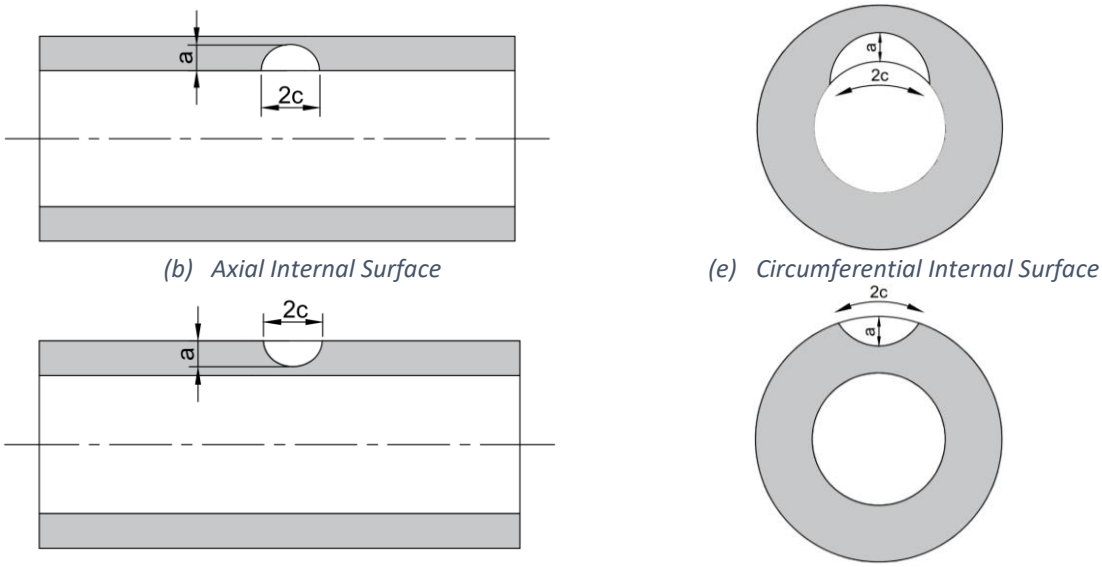

(b) Axial Internal Surface *(e) Circumferential Internal Surface*

(c) Axial External Surface *(f) Circumferential External Surface*

Figure 5: Flaw geometries for cylindrical specimens

Table 2: Tests analysed

Specimen Geometry	Reference	ID	Flaw Geometry	No. of Specimens Analysed
Wide Plate	[28]	302-306	SCT	1
			CCT	2
			ESCT	2
	[29]–[32]	702-716	SCT	6
	[33]	2507-2548	SCT	24
Closed Cylinder	[34]–[36]	721-728	Axial-External Surface	8
	[22]	1001-1003	Axial-External Surface	3
	[22]	1101-1107	Axial-External Surface	3
			Axial-Internal Surface	2
			Axial-Through thickness	1
	[37]	1201-1212	Axial-Through thickness	12
	[38]	1501-1503	Axial-External Surface	3
	[39]	1601-1604	Axial-External Surface	4
	[28]	2101-2102	Axial-External Surface	1
			Axial-Through thickness	1
	[40]	2103-2114	Axial-External Surface	7
			Axial-Internal Surface	1
			Axial-Through thickness	4
		2116-2133	Circumferential-External Surface	6
			Circumferential-Internal Surface	1
			Circumferential-Through Thickness	3
	[41]	2201-2292	Axial-Through thickness	88
		2301-2345	Axial-External Surface	33

Table 3: Validity limiting parameters of BS 7910 solutions for cylindrical geometries, specimens which exceed them and their parameter values

Flaw geometry	Cylinder Equation	Limiting parameter	Parameter value	Specimens exceeding limits
Axial-External Surface	M.7.2.4	0.1≤B/ri≤0.25	0.02-0.08	722-728, 1501-1503, 1601-1604, 2101, 2301-2345
		a/B≤0.8	0.80-0.81	2106, 2112, 2114
		0.05≤a/c≤1	≈0.048	2107, 2108, 2110
Axial-Internal Surface	M.7.2.2	a/B≤0.8	0.81	2109
Circumferential-Internal Surface	M.7.3.2	0.1≤a/c≤1	0.05	2125

Table 4: Cylinders assessed as Curved Shells

ID	Reference	Flaw Geometry	Specimens Analysed
722-728	[34]–[36]	Axial-External Surface	7
1501-1503	[38]	Axial-External Surface	3
1601-1604	[39]	Axial-External Surface	4
2301-2345	[41]	Axial-External Surface	33
2101	[28]	Axial-External Surface	1
2106-2108, 2110, 2112, 2114	[40]	Axial-External Surface	6
2109		Axial-Internal Surface	1
2125		Circumferential-Internal Surface	1

4. Results & Discussion

The following sections contain the results from all 212 analyses. They are divided in two categories according to the component geometry, i.e. wide plates and cylinders. Each category includes 37 and 175 specimens analysed respectively. The assessments were made with a single value of fracture toughness or with the use of a tearing resistance curve (R-curve), depending on the available data.

Each different material, and each test temperature, correspond to a different set of σ_y, σ_{UTS} values. Given that an FAL corresponds to a specific set of σ_y, σ_{UTS} values, this would result in a high number of FALs and FADs. In pursuit of brevity, the FADs presented in this section include two curves which correspond to the upper limit and lower limit of all the FALs of the specimens included in the graph. These were calculated by extracting from all the FALs, at each value of L_r, the maximum and minimum value of K_r that was calculated. There is no distinction between continuous and discontinuous yielding in these graphs since the main aim is to show that the assessment points of failed specimens lie outside the safe zone of the FALs.

Detailed reporting of the results of the analyses, the calculated values for the assessments and separate FADs for each set of tests can be found in [19].

4.1. Wide Plates

The results of the wide plate assessments are shown in Figure 6, where the blue and red markers refer to specimens which had surface flaws and through thickness flaws respectively. As explained previously (Section 3) some of the specimens included in the analyses, were either reported to not have reached failure or it was not clear whether the last values recorded during testing corresponded to failure, these are given as “unfailed specimens” and “uncertain failure” respectively.

In Figure 6, all the assessment points lie outside the minimum FAL, while specimens which didn’t fail during testing show a clear trend of being closer to the safe zone. These is a single specimen (ID:2518), that has been annotated and circled in Figure 6, which lies inside the maximum FAL. To address any initial concern regarding this specimen, Figure 7 gives the FAD containing the FAL that derives from the tensile properties of the material of 2518 at the respective test temperature. Figure 7 shows that it is assessed safely with the specimen lying outside the FAL in the unsafe zone.

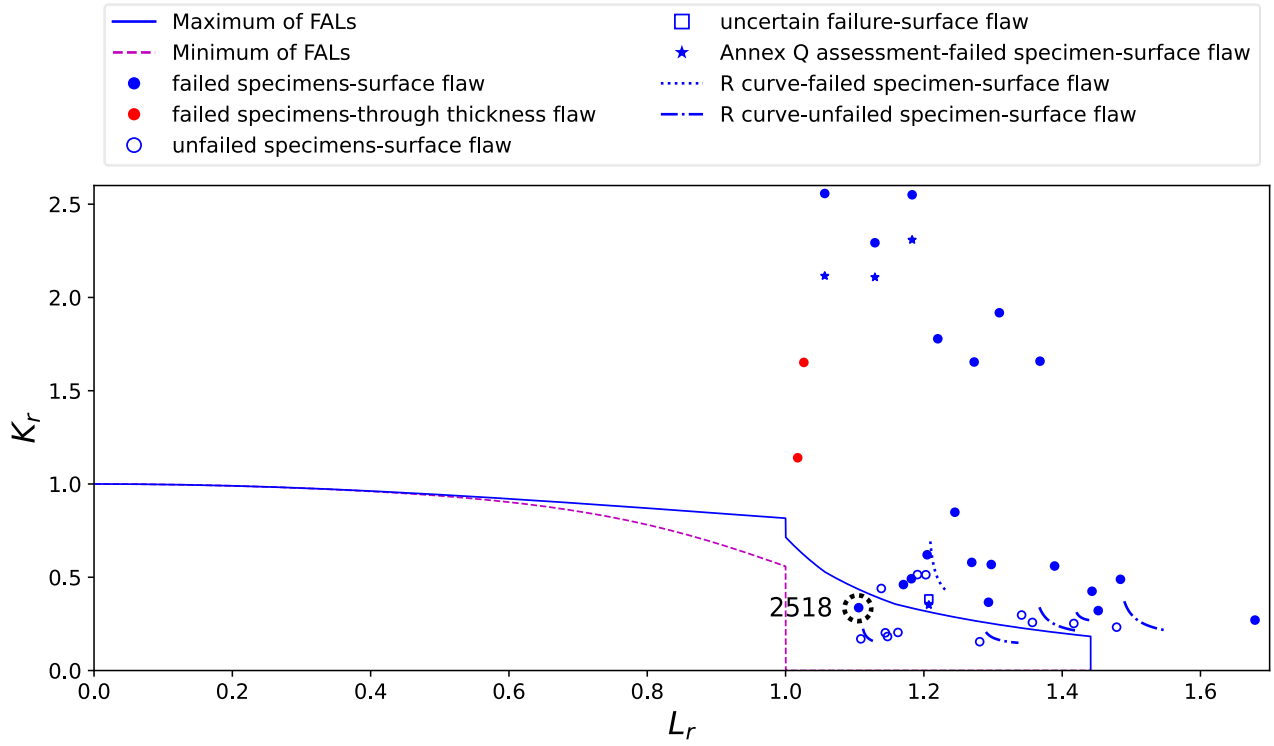

Figure 6: FAD of wide plate test data

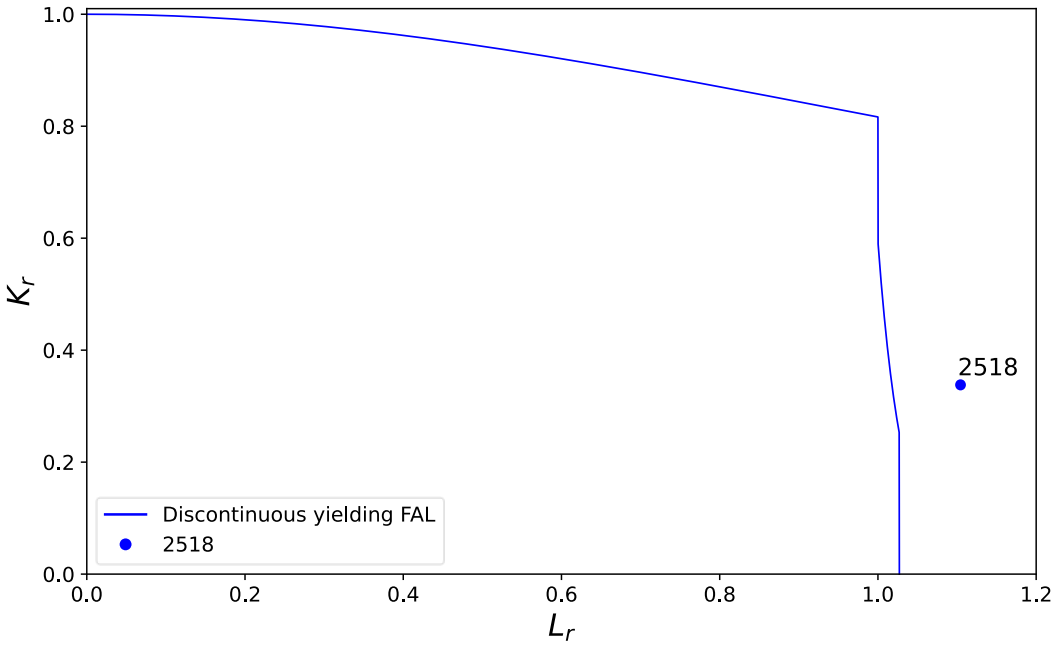

Figure 7: FAD of specimen 2518

4.2. Cylinders

4.2.1. Axially flawed

The assessment of all the axially flawed components has been conducted with the use of the reference stress equations of the 2019 version of the standard [1]. A comparison between the results using the equations from the 2013 and 2019 revisions of BS 7910 is given here in Figure 8, showing the decrease of conservatism between the different solutions, with the 2019 assessment points shifting closer to the FAL but remaining on the "unacceptable/unsafe" zone of the FAD. The decrease in conservatism comes from the decrease of the calculated L_r by approximately 20%, while the exact difference varies with the different values of K_r. A more detailed analysis of this comparison can be seen in [18], [19].

Figure 9 includes the results of this set of assessments conducted with the 2019 version of the standard. There, the blue and red points correspond to surface breaking and through thickness flawed specimens, respectively. Additionally, the open and closed points, denoted as "Charpy" and "K_{mat}" indicate whether fracture toughness values came from the use of Charpy measurements or fracture toughness testing, respectively. Following the conservatism in the formula used to calculate fracture toughness from Charpy measurements, it is observed in Figure 9 that the majority of Charpy based fracture toughness assessments lie further out from the FAL, in comparison to those based on fracture toughness testing.

In Figure 9 there is a single (circled) point lying in between the minimum and maximum of the FALs which corresponds to specimen 1602. This point together with the single R curve, of specimen 2113, lying very close to the FAL are given in Figure 10 a and b respectively. Figure 10 shows the assessment of the two specimens, i.e. 1602 and 2113, made using their respective tensile properties, where the assessment point/line lie outside both continuous and discontinuous yielding FALs. All of the above render the assessment procedure with the updated equations/reference stress solutions for pipes/curved shells, included in the 2019 version of the standard, safe.

Using curved shell SIF for cylinders, that lay outside the geometrical limits of the latter's K solutions is also supported in [25]. It appears from the results presented here that this action has given safe results without any trend of added conservatism. This could be an incentive to further research whether the limitations of the cylindrical geometry equations could be relaxed and still give safe results, however this would require a further parametric numerical and experimental study.

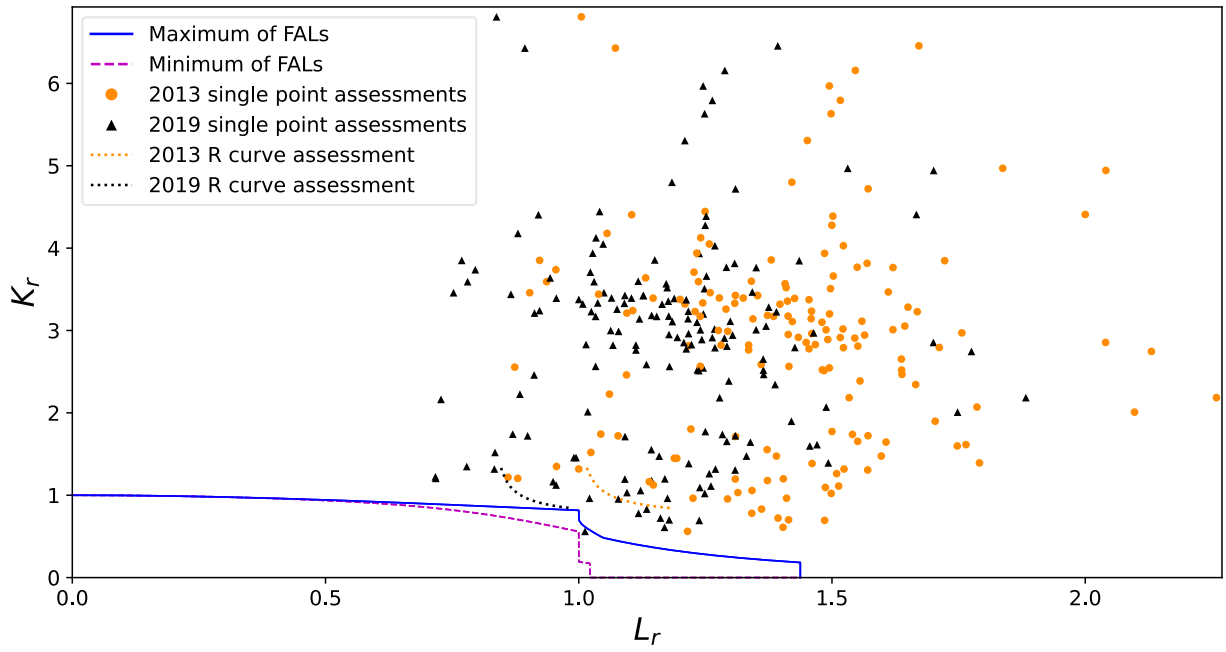

Figure 8: Comparison between BS7910 2013 and BS7910 2019 in assessing axially flawed cylinders

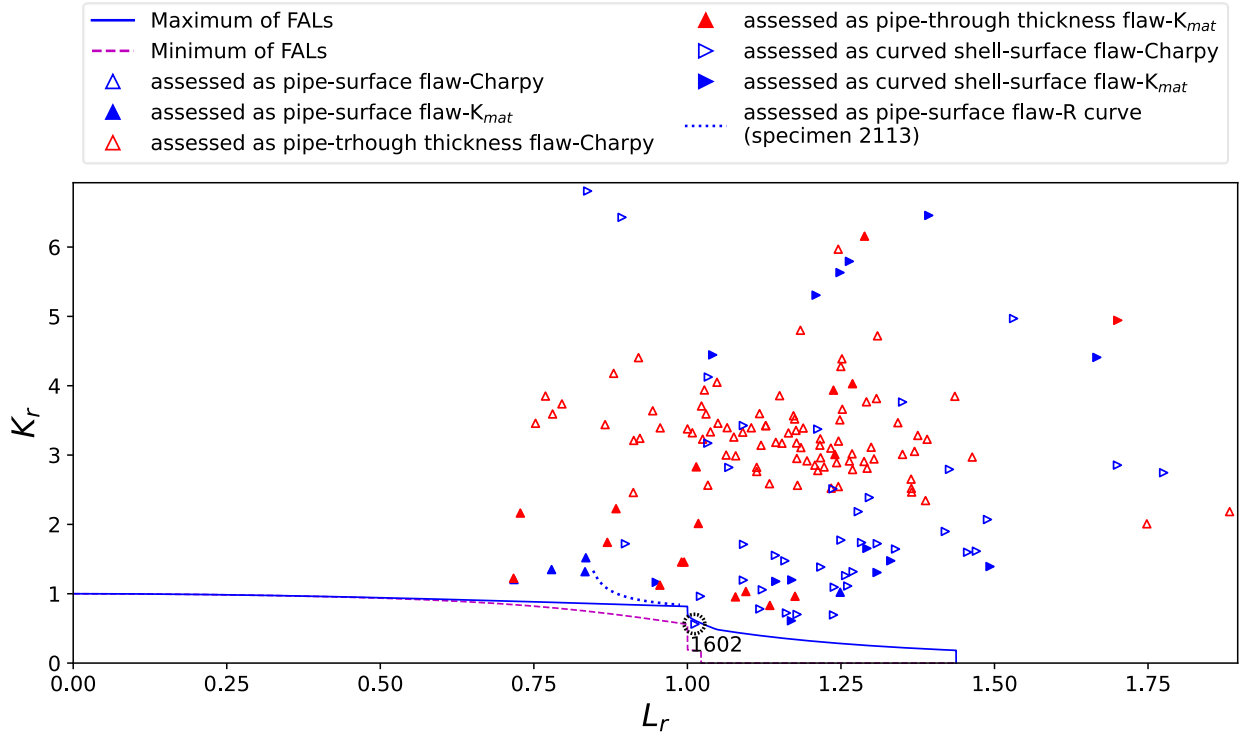

Figure 9: FAD of axially flawed cylinders (assessed with BS 7910 2019 version)

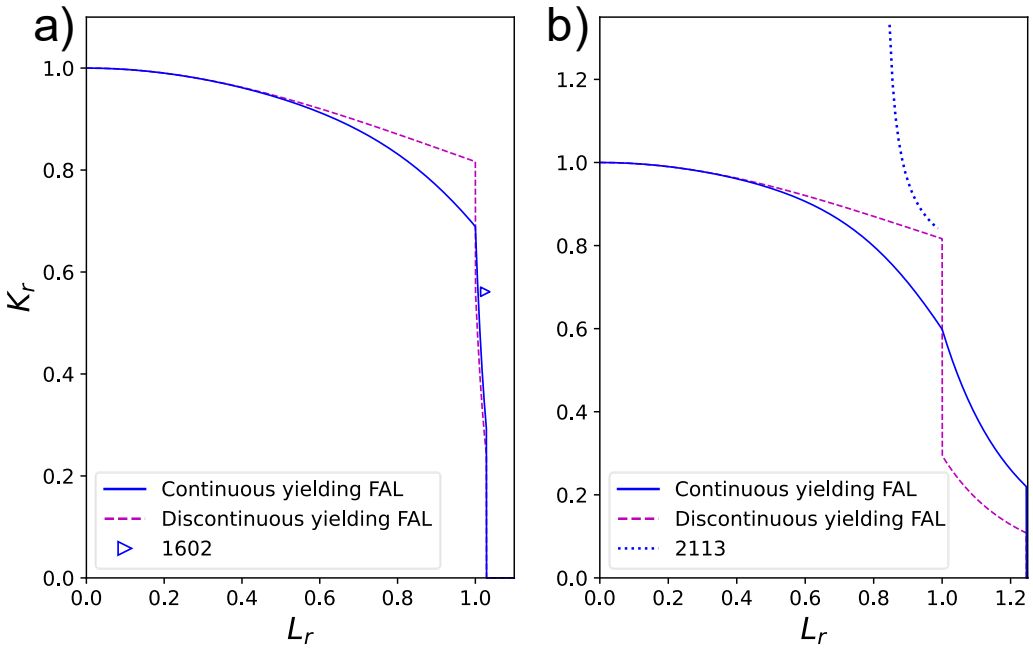

Figure 10: FAD of specimen a)1602, b)2113

4.2.2.Circumferentially flawed

The assessment results of the circumferentially flawed cylinders are shown in Figure 11, where again the blue and red coloured loci of points correspond to surface flawed and through thickness flawed specimens, respectively. Here all the assessments were made using tearing resistance curve data, which result in a locus of assessment points in the form of a line, as explained in section 2. Again, all the assessment points/lines lie outside the FALs.

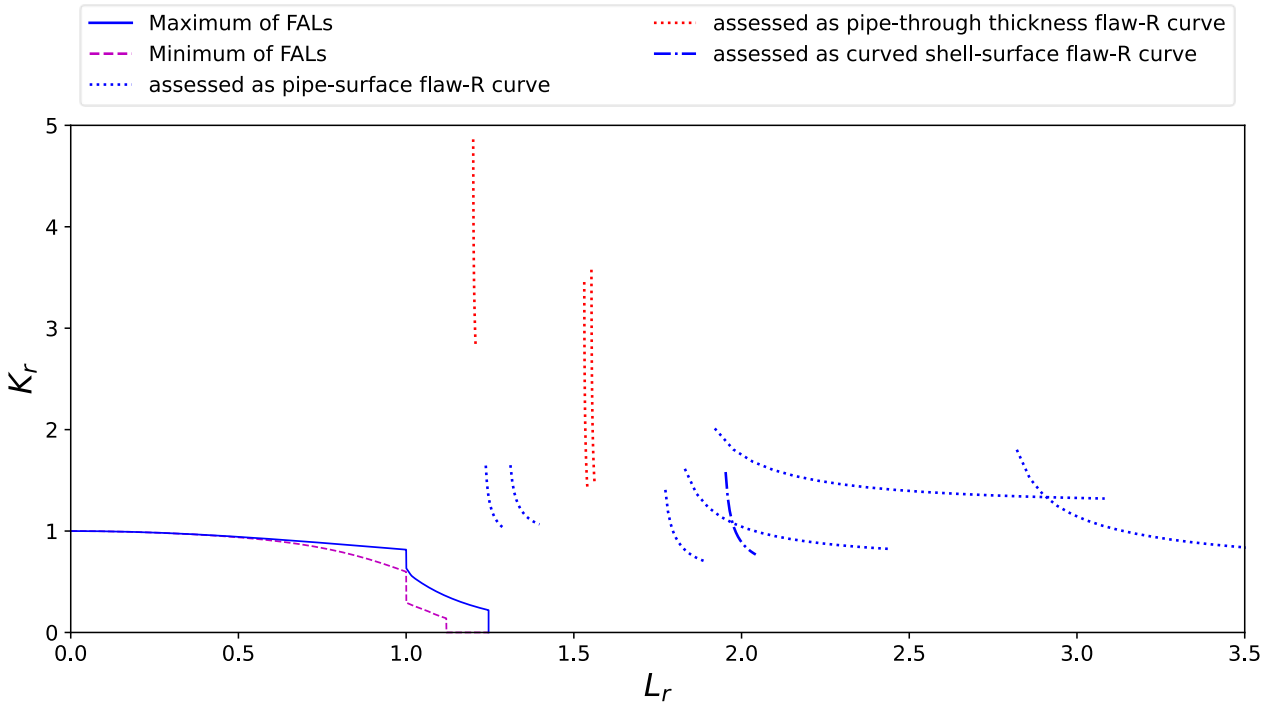

Figure 11: FAD of circumferentially flawed cylinders

5. Conclusions

A wide variety of large-scale tests were analysed in this work. From the results presented, BS 7910 and in particular its most conservative procedure, i.e. Option 1, can safely, albeit conservatively, estimate the fitness for service of a component and can predict failure. The level of this conservatism is something that might not be desired but is necessary for the procedure to be used in a fast manner, and multifunctionality of the procedure is mirrored in the high variation, between cases, of distance between the assessment point and the FAL.

It is important for procedures to be validated against experimental data, so they are calibrated against real cases. A characteristic example of the benefits of validating can be noted in this exercise. That is the pattern of unnecessary conservatism that had been observed on the reference stress solutions concerning cylinders/curved shells with axial through thickness, internal/external flaws. This regards a multiplication factor of 1.2 which was included in the previous version of the standard [17] and has been amended to 1 in the latest one [1], leading to a decrease of the calculated L_r by approximately 20%, while the exact difference in conservatism values varies with the different values of K_r. In this study the latest version of the reference stress solutions has been used, i.e. the factor has been 1. Further explanation of the history of this factor and the respective solutions included in other standards can be found in [18], while comparative results including both factors can be found in [18], [19].

One of the most important tasks accomplished here is re-gathering the experimental data. The data used here has been tracked back to the original reports in most cases. As expected, some reports were either unavailable or did not provide all the data needed, and data from earlier validation work was used and/or assumptions were accordingly made. Given the limited availability of such studies in the public domain an experimental database like the one constituted here is of very high value since it can be used for validation of future versions of both existing FFS standards and their constituents as well as new additions to them.

6. Acknowledgments

This work was made possible by the sponsorship of the industrial members of TWI as part of the Core Research Programme and of the UK Research and Innovation body. The work was enabled through the National Structural Integrity Research Centre (NSIRC), a postgraduate engineering facility for industry-led research into structural integrity established and managed by TWI through a network of both national and international Universities. Mahmoud Mostafavi acknowledges the Royal Academy of Engineering for financial support through a senior research fellowship.

7. Bibliography

[1] BSI, *BS 7910:2019 Guide to methods for assessing the acceptability of flaws in metallic structures*. BSi, 2019.

[2] EDF Energy Nuclear Generation Ltd., Ed., *Assessment of the Integrity of Structures Containing Defects, R6 - Revision 4 , as amended*. 2000.

[3] API, *API 579-1/ASME FFS-1 2016 Fitness-For-Service*. Washington, D.C.: American Petroleum Institute, 2016.

[4] A. J. Horn and A. H. Sherry, 'An engineering assessment methodology for non-sharp defects in steel structures – Part II: Procedure validation and constraint analysis', *Int. J. Press. Vessels Pip.*, vol. 89, pp. 151–161, Jan. 2012, doi: 10.1016/j.ijpvp.2011.10.015.

[5] C.-Y. Oh, H.-S. Nam, Y.-J. Kim, R. A. Ainsworth, and P. J. Budden, 'FE validation of R6 elastic–plastic J estimation for circumferentially cracked pipes under mechanical and thermal loadings', *Eng. Fract. Mech.*, vol. 124–125, pp. 64–79, Jul. 2014, doi: 10.1016/j.engfracmech.2014.03.015.

[6] R. D. Patel, ‘Validation of R6 using finite-element analyses of cracked cylinders under thermal loading’, *Nucl. Energy*, vol. 42, no. 05, pp. 257–262, 2003.
[7] Ş. E. Eren, T. London, Y. Yang, and I. Hadley, ‘Validation of Plastic Collapse Assessments Using BS 7910:2013 and R6 Procedures’, presented at the ASME 2013 Pressure Vessels and Piping Conference, Jan. 2014, doi: 10.1115/PVP2013-97513.
[8] I. Hadley, ‘BS 7910:2013 in brief’, *Int. J. Press. Vessels Pip.*, vol. 165, pp. 263–269, Aug. 2018, doi: 10.1016/j.ijpvp.2018.07.010.
[9] R. A. Ainsworth, P. J. Budden, A. R. Dowling, and J. K. Sharples, ‘Developments in the Flaw Assessment Procedures of R6 Revision 4 and BS7910’, Aug. 2008, pp. 19–25, doi: 10.1115/PVP2003-2023.
[10] B. R. Macejko, S. R. Kummari, and P. E. Prueter, ‘Proposed Modifications to API 579 Part 3 Brittle Fracture Screening Procedures’, in *Volume 1: Codes and Standards*, San Antonio, Texas, USA, Jul. 2019, p. V001T01A098, doi: 10.1115/PVP2019-93207.
[11] D. A. Osage and J. L. Janelle, ‘API 579-1/ASME FFS-1 2007: A Joint API/ASME Fitness-for-Service Standard for Pressurized Equipment’, in *Volume 1: Codes and Standards*, Chicago, Illinois, USA, Jan. 2008, pp. 777–791, doi: 10.1115/PVP2008-61796.
[12] D. A. Osage, B. Macejko, and R. G. Brown, ‘Proposed Modifications to API 579-1/ASME FFS-1 2007 Fitness-for-Service’, in *Volume 1: Codes and Standards*, Anaheim, California, USA, Jul. 2014, p. V001T01A002, doi: 10.1115/PVP2014-28451.
[13] C. Aird, ‘The R6 fracture procedure: an overview and summary of recent developments’, presented at the 15TH INTERNATIONAL CONFERENCE ON ENGINEERING STRUCTURAL INTEGRITY ASSESSMENT (ESIA15) + 2019 INTERNATIONAL SYMPOSIUM ON STRUCTURAL INTEGRITY (ISSI 2019), Cambridge, Under Publication.
[14] I. Hadley and P. Moore, ‘Fracture case studies for validation of fitness-for-service procedures’, TWI Ltd., Research Report 850/2006, May 2006.
[15] I. Hadley, ‘Validation of BS 7910:2013 and R6 Fracture Assessment Procedures: Uniaxial and Biaxial Wide Plate Tests on A533B Steel’, TWI Ltd., Members Report 1107/2018, Nov. 2018.
[16] J. Janelle, D. A. Osage, and S. J. Burkhart, ‘An Overview and Validation of the Fitness-For-Service Assessment Procedures for Local Thin Areas’, WRC (Welding Research Council inc.), Bulletin 505, 2005. Accessed: Mar. 31, 2020. [Online]. Available: https://www.forengineers.org/wrc-505.html.
[17] BSI, *BS 7910:2013+A1:2015 - Guide to methods for assessing the acceptability of flaws in metallic structures*. BSi, 2013.
[18] K. Kouzoumis, I. Hadley, and M. Mostafavi, ‘Validation of BS 7910; assessing the integrity of pipes containing axial flaws’, *Procedia Struct. Integr.*, vol. 13, pp. 868–876, Jan. 2018, doi: 10.1016/j.prostr.2018.12.165.
[19] I. Hadley, K. Kouzoumis, and Y. J. Janin, ‘Validation of BS 7910:2013 and R6 Fracture Assessment Procedures: Summary Report, Including Treatment of Plastic Collapse, Weld Strength Mismatch and Probabilistic Data [Appendix 1 available on request]’, TWI Ltd., Cambridge, TWI industrial member report 1125/2020, 2020.
[20] Y. Tkach and I. Hadley, ‘Reference Stress Solutions for Axial Flaws in Cylinders’, TWI Ltd., 13787/1/03, Dec. 2013.
[21] N. V. Challenger, R. Phaal, and S. J. Garwood, ‘Appraisal of PD 6493:1991 Fracture assessment procedures Part I: TWI data’, TWI Ltd., 512/1995, Jun. 1995.
[22] N. V. Challenger, R. Phaal, and S. J. Garwood, ‘Appraisal of PD 6493:1991 Fracture assessment procedures Part II: Published and additional TWI data’, TWI Ltd., 512/1995, Jun. 1995.
[23] I. Sattari-Far and F. Nilsson, ‘Validation of a procedure for safety assessment of cracks’, The Swedish Plant Inspectorate, Stockholm, SA/FoU-RAPPORT 90/04, Jun. 1990.
[24] I. Hadley and H. Pisarski, ‘Materials properties for Engineering Critical Assessment: Background to the advice given in BS 7910:2013’, *Int. J. Press. Vessels Pip.*, vol. 168, pp. 191–199, Dec. 2018, doi: 10.1016/j.ijpvp.2018.10.016.

[25] I. Hadley and Y. Lei, 'Outline of the fracture clauses of BS 7910:2013', *Int. J. Press. Vessels Pip.*, vol. 168, pp. 289–300, Dec. 2018, doi: 10.1016/j.ijpvp.2018.11.004.
[26] E. Lucon, K. Wallin, P. Langenberg, and H. Pisarski, 'The Use of Charpy/Fracture Toughness Correlations in the FITNET Procedure', in *24th International Conference on Offshore Mechanics and Arctic Engineering: Volume 3*, Halkidiki, Greece, Jan. 2005, pp. 365–368, doi: 10.1115/OMAE2005-67569.
[27] J. Sharples and I. Hadley, 'Treatment of residual stress in fracture assessment: background to the advice given in BS 7910:2013', *Int. J. Press. Vessels Pip.*, vol. 168, pp. 323–334, Dec. 2018, doi: 10.1016/j.ijpvp.2018.11.005.
[28] A. A. Willoughby and S. J. Garwood, 'Ductile fracture in thin section pipeline material.', TWI Ltd., Contract Report 3591/2/81, Oct. 1981.
[29] M. Brumovsky *et al.*, 'Analysis of the applicability of fracture mechanics on the basis of large scale specimen testing', Skoda, ZJE--281, 1988. Accessed: Feb. 09, 2018. [Online]. Available: http://inis.iaea.org/Search/search.aspx?orig_q=RN:20063256.
[30] J. Faleskog, K. Zaremba, F. Nilsson, and H. Öberg, 'An Investigation of Two-and Three Dimensional Elasto-Plastic Crack Growth Experiments', in *Defect Assessment in Components-Fundamentals and Applications*, London, 1991, pp. 333–343.
[31] D. Munz and S. Müller, 'Failure of components with surface cracks of the containment steel 15MnNi63', *Int. J. Press. Vessels Pip.*, vol. 30, no. 2, pp. 109–130, Jan. 1987, doi: 10.1016/0308-0161(87)90103-7.
[32] Y. Takahashi, N. Miura, and K. Kashima, 'Elastic-Plastic fracture analysis of surface cracks in pipe and plate by three-dimensional Finite Element Method', *ASME PVP*, vol. 167, pp. 63–69, 1989.
[33] A. C. Bannister and Trail, 'SUB-TASK 2.3: YIELD STRESS/TENSILE STRESS RATIO: RESULTS OF EXPERIMENTAL PROGRAMME', British Steel, RUG, UC, SINTAP/BS/25, Feb. 1999.
[34] W. Brocks, G. Künecke, and K. Wobst, 'Stable crack growth of axial surface flaws in pressure vessels', *Int. J. Press. Vessels Pip.*, vol. 40, no. 1, pp. 77–90, Jan. 1989, doi: 10.1016/0308-0161(89)90125-7.
[35] H. P. Keller, G. Junker, and W. Merker, 'Fracture analysis of surface cracks in cylindrical pressure vessels applying the two parameter fracture criterion (TPFC)', *Int. J. Press. Vessels Pip.*, vol. 29, no. 2, pp. 113–153, Jan. 1987, doi: 10.1016/0308-0161(87)90121-9.
[36] I. Milne and N. Knee, 'An EGF Exercise in predicting ductile instability : Phase 2, Cracked pressure vessel', Central Electricity Generating Board, CEGB-TPRD/L/2771/N84, Jun. 1986.
[37] C. A. Sciammarella, 'Elastic-Plastic failure analysis of pressure vessel tests', *Fract. Mech. Fourteenth Symp.*, pp. 597–616, Jan. 1985.
[38] W. Sloterdijk, 'The influence of the yield-to-tensile ratio on deformation controlled pipeline behaviour', presented at the PRC/EPRG 10th Biennial Joint Technical Meeting on Line Pipe research, Cambridge, Nov. 1995.
[39] G. Demofonti, G. Mannucci, D. Harris, L. Barsanti, and H.-G. Hillenbrand, 'Fracture behaviour of X100 gas pipelines by full-scale tests', Yokohama, Japan, Nov. 2002, pp. 245–261.
[40] D. Sturm and W. Stoppler, 'Phenomenological Pipe and Vessel Burst Tests', MPA, Stuttgart, Project 1500 279, 1989.
[41] J. Kiefner, W. Maxey, R. Eiber, and A. Duffy, 'Failure Stress Levels of Flaws in Pressurized Cylinders', Jan. 1973, doi: 10.1520/STP49657S.
[42] M. F. Kanninen *et al.*, 'Instability predictions for circumferentially cracked type 304 stainless steel pipes under dynamic loading', EPRI, Palo Alto, NP-2347, 1982.